AGU PUBLICATIONS

Space Weather

RESEARCH ARTICLE
10.1002/2014SW001033

Key Points:
- This study is for the improvement of empirical geomagnetic storm forecast
- We use the initially observed CME parameters as the first step of the forecast
- We also use the solar wind parameters for near-real forecast

Correspondence to:
R.-S. Kim,
rskim@kasi.re.kr

Citation:
Kim, R.-S., Y.-J. Moon, N. Gopalswamy, Y.-D. Park, and Y.-H. Kim (2014), Two-step forecast of geomagnetic storm using coronal mass ejection and solar wind condition, *Space Weather*, *12*, 246–256, doi:10.1002/2014SW001033.

Received 6 JAN 2014
Accepted 24 MAR 2014
Accepted article online 28 MAR 2014
Published online 14 APR 2014

Two-step forecast of geomagnetic storm using coronal mass ejection and solar wind condition

R.-S. Kim[1], Y.-J. Moon[2], N. Gopalswamy[3], Y.-D. Park[1], and Y.-H. Kim[1]

[1]Astronomy and Space Program Division, Korea Astronomy and Space Science Institute, Daejeon, South Korea, [2]School of Space Research, Kyung Hee University, Yongin, South Korea, [3]Heliophysics Division, Goddard Space Flight Center, Greenbelt, Maryland, USA

Abstract To forecast geomagnetic storms, we had examined initially observed parameters of coronal mass ejections (CMEs) and introduced an empirical storm forecast model in a previous study. Now we suggest a two-step forecast considering not only CME parameters observed in the solar vicinity but also solar wind conditions near Earth to improve the forecast capability. We consider the empirical solar wind criteria derived in this study ($B_z \leq -5$ nT or $E_y \geq 3$ mV/m for $t \geq 2$ h for moderate storms with minimum *Dst* less than −50 nT) and a *Dst* model developed by Temerin and Li (2002, 2006) (TL model). Using 55 CME-*Dst* pairs during 1997 to 2003, our solar wind criteria produce slightly better forecasts for 31 storm events (90%) than the forecasts based on the TL model (87%). However, the latter produces better forecasts for 24 nonstorm events (88%), while the former correctly forecasts only 71% of them. We then performed the two-step forecast. The results are as follows: (i) for 15 events that are incorrectly forecasted using CME parameters, 12 cases (80%) can be properly predicted based on solar wind conditions; (ii) if we forecast a storm when both CME and solar wind conditions are satisfied (∩), the critical success index becomes higher than that from the forecast using CME parameters alone, however, only 25 storm events (81%) are correctly forecasted; and (iii) if we forecast a storm when either set of these conditions is satisfied (∪), all geomagnetic storms are correctly forecasted.

1. Introduction

Geomagnetic storms are caused by disturbances in the interplanetary (IP) medium. The storms are defined by changes in the *Dst* (disturbance storm time) index, which estimates the globally averaged change of the horizontal component of the Earth's magnetic field at the magnetic equator. During the geomagnetic storm, severe changes occur both in IP space and the terrestrial environment such as the acceleration of charged particles and the enhancement of electric currents, auroras, and magnetic field variations on the Earth's surface, which can endanger human life or health [*Schwenn*, 2006]. Therefore, the forecast of geomagnetic storms is a key aspect of space weather science and one of the most important subjects in solar-terrestrial physics. For this reason, we derived methods to forecast moderate storms with minimum *Dst* less than −50 nT in previous studies [*Kim et al.*, 2005, 2008, 2010].

According to *Gonzalez et al.* [1994], geomagnetic storms can be defined in terms of their intensity by *Dst* minimum value as follows: (1) weak or minor storm, minimum *Dst* falls between −30 and −50 nT; (2) moderate storm, minimum *Dst* falls between −50 and −100 nT; and (3) strong storm, minimum *Dst* is −100 nT or less. Most researches have examined intense storms with minimum *Dst* less than −100 nT, since they have clear solar sources that are easy to find. According to NOAA space weather scale, the moderate geomagnetic storms can also affect the modern technology, and they occur more frequently than intense storms. *Zhang et al.* [2006] reported that the occurrence rate of weak storms is much higher than that of strong storms, especially early in the solar minimum phase.

The storm forecast can be roughly classified into an urgent warning about 1 h in advance using spacecraft measurements at the L1 point [*Temerin and Li*, 2002, 2006; *Wang et al.*, 2003; *Boynton et al.*, 2011] and a medium-term forecast from several hours to several days ahead [*Srivastava and Venkatakrishnan*, 2004; *Kim et al.*, 2005, 2008, 2010; *Song et al.*, 2006; *Kang et al.*, 2006]. In case of the urgent warning, the forecasts are rather exact (~90%), but the alert time (ΔT < 1 h) is too short for practical aims. For the medium-term forecast, coronal mass ejections (CMEs) and their associated shock waves are very important as they can

compress the magnetosphere and trigger geomagnetic storms [*Brueckner et al.*, 1998; *Gopalswamy et al.*, 2000; *Cho et al.*, 2010]. The forecasts based on initially observed CME parameters are very useful for practical purposes because they give us the time about 2–3 days in advance to prepare for the geomagnetic storms.

One of the main concerns faced by the medium-term forecast is to predict the arrival time of a CME at the Earth [*Gopalswamy et al.*, 2001; *Moon et al.*, 2002; *Cho et al.*, 2003; *McKenna-Lawlor et al.*, 2006; *Kim et al.*, 2007]. *Gopalswamy et al.* [2001] developed an empirical CME arrival model to predict the 1 AU arrival of Earth-directed CMEs using coronagraphic and in situ observations. The main input parameter to this model is the initial speed of the CMEs obtained remotely by white light observations. The other concern is to predict the occurrence and magnitude of an ensuing geomagnetic storm as the CME arrives. *Kim et al.* [2010] developed an empirical model to forecast geomagnetic storm occurrence and strength, given by minimum *Dst*, solely based on initially observed CME parameters. They evaluated the model by comparing predicted and observed storm occurrences. However, the forecast using CME parameters has some limitations. For example, the plane-of-sky speed can produce an error in predicted storm occurrence time. And the CME parameters such as the direction of the CMEs propagation and the magnetic field orientation of the interplanetary CMEs (ICMEs, when CMEs arrive at the Earth), which are assumed to remain the same throughout CMEs propagation, may change. CMEs can interact with the surrounding background solar wind as they propagate away from the Sun. Many CMEs slow down as they travel from the Sun out to 1 AU. *Wu and Lepping* [2002] found that a geomagnetic storm can be induced by a sheath and a trailing part as well as the ICME itself. It is needed to study more about the interactions between the magnetosphere and different regions in the ICME. Due to those limitations, the accuracy of medium-term forecasts remains rather poor.

Therefore, to improve the forecast capability of geomagnetic storms, we may need to combine medium-term forecast with the urgent warning based on IP measurements. *Gonzalez and Tsurutani* [1987] showed that 10 intense magnetic storms (minimum $Dst \leq -100$ nT) were caused by large and negative (< -10 nT) interplanetary magnetic fields (IMF B_z) associated with IP duskward electric field ($E_y > 5$ mV/m) lasting for 3 h. From this result, they suggested this condition as the criteria for intense storms. *Echer et al.* [2008] also showed the relation between the *Dst* index and IP parameters, such as magnetic field, electric field, and energy transferred from the solar wind to the magnetosphere using superintense geomagnetic storms (minimum $Dst \leq -250$ nT) during Solar Cycle 23. Another way to forecast a storm with IP data is to use a model that predicts the *Dst* index directly. *Ji et al.* [2012] evaluated *Dst* forecast models to explore suitable models for real-time space weather forecast. Among several models based on solar wind and *Dst* data [*Burton et al.*, 1975; *Fenrich and Luhmann*, 1998; *O'Brien and McPherron*, 2000; *Temerin and Li*, 2002, 2006; *Wang et al.*, 2003; *Boynton et al.*, 2011], they found that the model of *Temerin and Li* [2002, 2006] (hereafter TL model) gave the best forecast result for strong storms ($-100 \leq$ minimum $Dst < -200$ nT).

In this study, we suggest new solar wind criteria as the second step of a geomagnetic storm forecast by examining two different approaches. One is modifying the Gonzalez and Tsurutani (GT) criteria for moderate storms (minimum $Dst \leq -50$ nT), and the other is using the TL model. Then we combine those results with the first step of the forecast, which is based on CME parameters. That is, after the storm forecast using only initially observed CME parameters, we perform a forecast again using the solar wind data as the second step. We expect that this combined process of two-step forecast can significantly improve the storm forecast capability.

The paper is organized as follows. Data and methodology of our study are given in section 2. We examine the relationship between *Dst* index and solar wind parameters and suggest new criteria of solar wind parameters in section 3. We also compare the statistical results of each forecast from CME parameters, solar wind criteria, and the *Dst* model. Then we present several methods to combine the two forecast domains to produce a two-step forecast in section 4. A brief summary and discussion are presented in section 5.

2. Data and Methodology

2.1. Forecast Models Using CME Parameters

We use the CME list from *Kim et al.* [2010], which contains 66 events from 1997 to 2003. They selected only halo CME events associated with M or X class flares with clearly identified source regions on the Sun. They listed CME location and speed observed by the Large Angle Spectroscopic Coronagraph (LASCO) [*Brueckner et al.*, 1995] on board the Solar and Heliospheric Observatory. They calculated the direction parameter (D), which shows how much CME propagation is directed the Earth. The direction parameter

is designed to be one when a CME is exactly propagating along the Sun-Earth line. To perform the medium-term forecast, we also need the magnetic field direction in the CMEs' initial phase, since the southward magnetic field direction of ICMEs is the essential parameter for the geomagnetic storm occurrence [*Bothmer and Schwenn*, 1998]. Although the magnetic fields inside the CMEs can be changed during their propagation, the directions (south or north) are seldom changed [*Yurchyshyn et al.*, 2009]. We estimate the magnetic field direction of CMEs based on the magnetic field orientation angle (θ) of associated active region on the solar surface. This value is from the potential field model, which is the extrapolation of the photospheric measurements upward into the corona magnetic connectivity [*Song et al.*, 2006]. If the magnetic field orientation angle is less than 90°, the direction of the magnetic field orientation is southward; otherwise, the orientation is northward. To avoid ambiguity, we use only well-isolated events by excluding 10 multiple events and 1 event with a solar wind data gap. Table 1 shows the information for 55 CMEs. The first three columns display the CME's observing date and time, plane-of-sky speed, and direction parameter [*Yashiro et al.*, 2004; *Moon et al.*, 2005, 2009; *Kim et al.*, 2008]. The fourth and the fifth columns give the location and the magnetic field orientation angle of the associated active region (AR).

The sixth column of the table shows the expected CME arrival time based on the empirical CME arrival model suggested by *Gopalswamy et al.* [2001]. It calculates the arrival time of CMEs using linear speeds and first appearance times in the LASCO C2 or C3 field of view. For the forecast of storm strength, we use the empirical formulae developed by *Kim et al.* [2010], which are expressed by

$$Dst(\mathrm{nT}) = 172 - 199 \times V - 337 \times D \tag{1}$$

for southward events and

$$Dst(\mathrm{nT}) = 47 + 53 \times L - 47 \times V - 202 \times D \tag{2}$$

for northward events. Here the southward event represents a CME that has southward magnetic field orientation in its source region ($\theta \leq 90°$), and the northward event has northward magnetic field orientation ($\theta > 90°$). The CME parameters, location (L), speed (V), and direction parameter (D) are all normalized to their maxima so that their values always lie between 0 and 1. We list the expected storm strength in the seventh column of the table.

2.2. Solar Wind Condition and TL Model

To examine solar wind condition during geomagnetic storms, we use OMNI data from the Coordinated Data Analysis (Workshop) Web [*King and Papitashvili*, 2005]. The data set consists of hourly averaged definitive multispacecraft (mainly ACE (Advanced Composition Explorer) and Wind) solar wind parameters at 1 AU including magnetic field magnitude (B_x, B_y, B_z), electric field (E_y), ion number density (N_i), flow dynamic pressure (P_{dyn}), plasma flow speed (V_{SW}), and plasma temperature (T). It also provides the *Dst* index from the World Data Center operated by the Data Analysis Center for Geomagnetism and Space Magnetism in Kyoto University. Figure 1 shows the time profiles of solar wind parameters and the *Dst* index. Two vertical solid lines indicate CME occurrence time (06:10 UT on 4 November 1997) and expected CME arrival time at the Earth (13:39 UT on 7 November 1997) from an empirical model [*Gopalswamy et al.*, 2001], respectively. Two dotted vertical lines represent a ±24 h time window from the predicted CME arrival time. As shown in Figure 1a, a disturbance of solar wind parameters was observed at 00:30 UT on 7 November in all solar wind data, and the *Dst* index started to decrease and reached the minimum value of −110 nT at 04:30 UT as marked by blue line in Figure 1b. The predicted minimum *Dst* in this case was only −43 nT compared to the observed −110 nT representing a miss in the prediction of a storm event using CME parameters. In addition, the predicted time of *Dst* minimum was 9 h later than the observed.

To determine the strength of the disturbance in each parameter, we find the maximum (or minimum) values in the time window, which starts at 24 h before the expected CME arrival time and ends on the real *Dst* minimum time. We list the minimum B_z and maximum E_y for each event in the eighth and the ninth columns of Table 1. We also measure the duration of the disturbance before *Dst* minimum. In the table, we include the durations in parentheses, in which B_z or E_y stay in certain ranges ($B_z \leq -5$ nT and $E_y \geq 3$ mV/m). We will explain these criteria in section 3.2.

For practical usage, we also examine the predicted *Dst* values from the TL model, which are calculated by the sum of three terms, such as the dynamic pressure, interplanetary magnetic field, and some offsets. The

Table 1. Information of 55 CME-*Dst* Pairs From 1997 to 2003

CME			AR		Forecast Model		Solar Wind			Observed *Dst* Minimum	
Date/Time	*V* (km/s)[a]	*D*	Location	MFO (°)[b]	Arrival	*Dst* (nT)	B_z (nT)	E_y (mV/m)	TL Model (nT)	Time	Intensity (nT)
1997/11/04 06:10	785	0.42	S14W33	90.48	11/07 13:39	−43	−12.2 (3)	5.8 (3)	−105	11/07 04	−110
1998/04/29 16:58	1374	0.54	S18E20	86.13	05/01 09:29	−119	−8.4 (1)	3.4 (1)	−29	05/02 07	−24
1998/05/02 14:06	938	0.58	S15W15	46.81	05/05 07:42	−98	−9.6 (3)	7.8 (2)	−201	05/05 04	−119
1998/11/05 20:44	1118	0.40	N22W18	91.52	11/08 01:29	−53	−11.7 (7)	12.3 (8)	−144	11/08 06	−149
1998/11/27 08:30	434	0.75	S24E09	78.46	12/01 14:19	−115	−8.0 (1)	3.3 (1)	−29	12/01 16	−26
1999/05/03 06:06	1584	0.15	N17E32	90.01	05/04 15:55	10	−1.1 (0)	0.9 (0)	−14	05/03 21	−20
1999/05/10 05:50	920	0.15	N16E19	20.94	05/13 00:57	48	−10.7 (2)	4.5 (2)	−46	05/13 14	−49
1999/06/26 07:31	558	0.60	N25E00	102.20	06/30 09:03	−77	−2.0 (0)	1.1 (0)	−10	06/29 21	−17
1999/06/29 18:54	438	0.56	S15E01	102.89	07/04 00:38	−66	−5.4 (1)	2.9 (0)	−25	07/03 12	−25
1999/06/30 11:54	406	0.80	S15W03	21.38	07/04 18:13	−129	1.1 (0)	−0.5 (0)	−16	07/03 18	−17
1999/07/28 09:06	462	0.65	S15E03	15.47	08/01 14:16	−83	−6.0 (2)	3.6 (2)	−40	07/31 23	−39
1999/10/14 09:26	1250	0.49	N11E32	142.81	10/16 07:09	−51	0.6 (0)	0.0 (0)	−44	10/15 07	−50
1999/12/22 02:30	570	0.38	N10E27	105.58	12/26 03:23	−19	−2.3 (0)	1.4 (0)	−14	12/25 08	−8
1999/12/22 19:31	605	0.39	N24E19	99.53	12/26 18:18	−25	−4.1 (0)	1.2 (0)	−4	12/27 01	−8
2000/01/18 17:54	739	0.58	S19E11	152.69	01/22 05:44	−70	−16.0 (8)	5.7 (7)	−109	01/23 00	−97
2000/02/08 09:30	1079	0.43	N25E26	71.21	02/10 16:41	−58	−3.4 (0)	2.8 (0)	−25	02/11 12	−25
2000/02/12 04:31	1107	0.46	N26W23	83.14	02/14 09:57	−71	−7.2 (2)	4.5 (2)	−59	02/14 13	−67
2000/02/17 20:06	600	0.46	S29E07	42.61	02/21 19:12	−30	−7.8 (1)	2.9 (0)	−26	02/21 20	−26
2000/06/06 15:54	1119	0.82	N20E18	78.22	06/08 20:36	−193	−7.1 (3)	5.3 (4)	−74	06/08 19	−90
2000/06/07 16:30	842	0.73	N23E03	73.98	06/10 18:36	−141	−5.5 (2)	3.2 (1)	−37	06/10 07	−52
2000/06/10 17:08	1108	0.42	N22W38	115.03	06/12 22:20	−47	−4.9 (0)	2.3 (0)	−29	06/13 12	−37
2000/07/11 13:27	1078	0.52	N18E27	8.52	07/13 20:43	−89	−2.3 (0)	4.5 (1)	−37	07/13 21	−43
2000/07/14 10:54	1674	0.75	N22W07	17.31	07/15 18:28	−214	−49.3 (5)	51.4 (6)	−251	07/16 00	−301
2000/07/25 03:30	528	0.69	N06W08	58.38	07/29 06:26	−102	−11.9 (4)	5.3 (3)	−70	07/25 11	−71
2000/09/12 11:54	1550	0.56	S17W09	113.57	09/13 22:39	−92	−4.6 (0)	1.6 (0)	−47	09/13 02	−45
2000/09/16 05:18	1215	0.80	N14W07	52.68	09/18 04:43	−194	−23.0 (4)	14.9 (4)	−216	09/17 23	−201
2000/11/24 05:30	994	0.58	N20W05	41.29	11/26 18:39	−102	−10.8 (3)	6.2 (3)	−60	11/27 01	−80
2000/11/25 19:31	671	0.72	N20W23	38.88	11/29 13:23	−124	−12.0 (13)	5.6 (10)	−100	11/29 13	−119
2001/01/20 19:31	839	0.45	S07E40	42.12	01/23 21:54	−46	−6.8 (9)	2.9 (0)	−44	01/24 18	−61
2001/03/24 20:50	906	0.74	N15E22	64.38	03/27 17:09	−149	−17.4 (4)	4.7 (2)	−75	03/28 15	−87
2001/03/28 01:27	427	0.72	S08E50	88.65	04/01 07:25	−104	−33.3 (7)	21.4 (8)	−411	03/31 21	−284
2001/03/29 10:26	942	0.94	N20W19	7.16	04/01 03:42	−219	−46.3 (4)	30.6 (4)	−411	03/31 08	−387
2001/04/06 19:30	1270	0.65	S21E31	60.30	04/08 16:18	−148	−4.6 (0)	3.8 (1)	−52	04/09 06	−63
2001/04/09 15:54	1192	0.69	S21W04	82.10	04/11 16:30	−155	−17.7 (2)	14.9 (5)	−228	04/11 23	−271
2001/04/11 13:31	1103	0.61	S22W27	87.12	04/13 19:12	−121	−6.3 (1)	5.7 (1)	−90	04/13 15	−77
2001/04/26 12:30	1006	0.30	N17W31	41.79	04/29 00:46	−9	−12.3 (11)	4.9 (6)	−82	04/29 02	−47
2001/08/25 16:50	1433	0.23	S17E34	22.59	08/27 07:13	−19	−7.4 (1)	2.4 (0)	−23	08/26 08	−25
2001/09/24 10:30	2402	0.37	S16E23	62.13	09/25 06:56	−143	−10.3 (2)	4.3 (2)	−31	09/26 01	−102
2001/09/28 08:54	846	0.69	N10E18	51.66	10/01 10:38	−127	−10.3 (5)	6.2 (8)	−136	10/01 08	−148
2001/10/09 11:30	973	0.53	S28E08	116.29	10/12 02:17	−66	−11.7 (2)	7.1 (1)	−93	10/12 12	−71
2001/10/19 16:50	901	0.62	N15W29	122.39	10/22 13:36	−88	−12.8 (5)	10.6 (3)	−176	10/21 21	−187
2001/10/28 00:26	592	0.42	N12E45	62.98	11/01 00:02	−16	−12.3 (15)	5.0 (14)	−95	11/01 10	−106
2001/11/04 16:35	1810	0.77	N06W18	50.73	11/05 21:15	−231	−61.0 (4)	- (-)	−229	11/06 06	−292
2001/11/28 17:30	500	0.45	N04E16	76.64	12/02 21:31	−19	−10.1 (3)	3.9 (2)	−16	12/03 21	−32
2002/03/15 23:06	907	0.61	S08W03	30.62	03/18 19:20	−105	−10.6 (2)	4.2 (2)	−60	03/19 06	−37
2002/04/15 03:50	720	0.86	S15W01	21.35	04/18 17:25	−175	−12.2 (7)	6.6 (7)	−122	04/18 07	−127
2002/04/17 08:26	1218	0.49	S14W34	30.97	04/19 07:42	−90	−13.9 (4)	8.4 (6)	−135	04/20 06	−148
2002/07/15 20:30	1132	0.39	N19W01	91.06	07/18 00:25	−45	−4.2 (0)	2.2 (0)	−18	07/18 11	−17
2002/07/18 08:06	1099	0.22	N19W30	91.47	07/20 14:01	−10	−5.8 (1)	4.3 (2)	−40	07/20 23	−34
2002/07/26 22:06	818	0.41	S19E26	158.02	07/30 02:27	−30	−2.4 (0)	0.9 (0)	−13	07/29 08	−14
2002/08/16 12:30	1459	0.41	S14E20	57.50	08/18 02:01	−82	−5.4 (3)	3.5 (2)	−48	08/19 01	−47
2002/12/19 22:06	1092	0.55	N25W18	98.46	12/22 04:27	−83	−1.8 (0)	0.6 (0)	−76	12/21 14	−48
2003/05/27 23:50	964	0.83	S07W17	141.31	05/30 15:19	−137	−11.6 (2)	9.6 (6)	−136	05/29 23	−144
2003/10/28 11:30	2459	0.94	S16E08	171.15	10/29 07:22	−177	−24.6 (10)	- (-)	−303	10/30 00	−353
2003/10/29 20:54	2029	0.83	S15W02	76.32	10/30 21:51	−269	−28.2 (3)	- (-)	−400	10/30 22	−383

[a]Linear speed.
[b]Magnetic field orientation in the solar source region. Southward events have smaller angles than 90°.

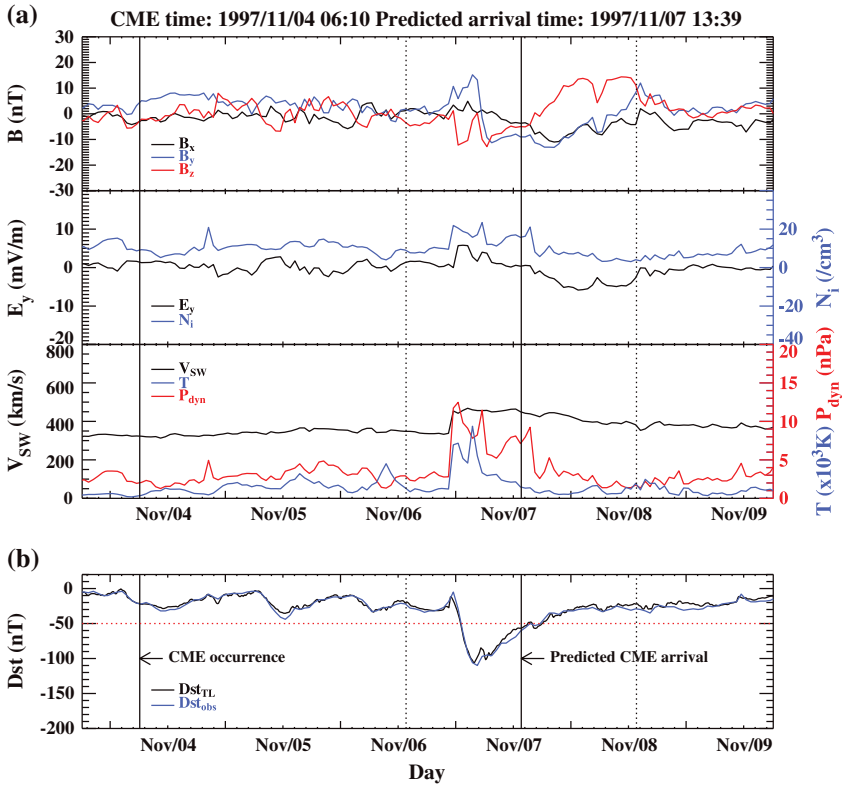

Figure 1. (a) Time profiles of solar wind parameters and (b) observed and estimated *Dst* indices corresponding to a CME occurred at 06:10 UT on 4 November 1997. Two vertical solid lines indicate CME appearance time in the LASCO field of view and predicted arrival time at the Earth, respectively. Two vertical dotted lines delineate the ±24 h time window of the predicted CME arrival time at the Earth.

model starts running within 2 min of new solar wind data appearing on the ACE web site, and the time step of predictions is 10 min; therefore, we can expect around 1 h lead time depending on the speed of the solar wind. The real-time prediction of the *Dst* index is distributed through the internet (http://lasp.colorado.edu/space_weather/dsttemerin/dsttemerin.html). In Figure 1b, it is shown that the predicted *Dst* index from the TL model agrees well with the observed *Dst* index as illustrated by black and blue solid lines, respectively. We list the minimum values of the modeled *Dst* index within the ±24 h time window of the expected CME arrival time in the tenth column of Table 1. The last two columns in the table are the observed *Dst* minimum time and intensity. In this study, we define geomagnetic storms when the *Dst* minimum is below −50 nT so that 31 CMEs are found to be geoeffective among 55 events, and the mean probability of CME geoeffectiveness is about 56%.

3. Geomagnetic Storm Forecasts Using Solar Wind Data

3.1. Relation Between *Dst* Index and Solar Wind Parameters

To select storm criteria of solar wind parameters, we examine their relationship with the minimum *Dst* index as shown in Figure 2. For the magnetic field strength, we consider all six components (positive B_x, B_y, B_z and negative B_x, B_y, B_z) to see which direction of solar wind magnetic field is more related to the storm intensity. In Figure 2 (left column), the open circles represent the maximum values of magnetic field strength in the positive direction and filled circles are the maximum values in the negative direction. It is clearly seen that the strong storms have strong magnetic fields, and we find that the negative B_z has the best relationship with the minimum *Dst* with the highest correlation coefficient of 0.84 among six magnetic field components. As shown in the right column of the figure, IP duskward electric field (E_y) also has good correlation with the minimum *Dst* (cc = −0.85). However, other parameters such as the ion number density (N_i) and the plasma temperature (T) do not show strong relationships. These results are consistent with other research [*Yermolaev et al.*, 2007; *Echer et al.*, 2008; *Ji et al.*, 2010].

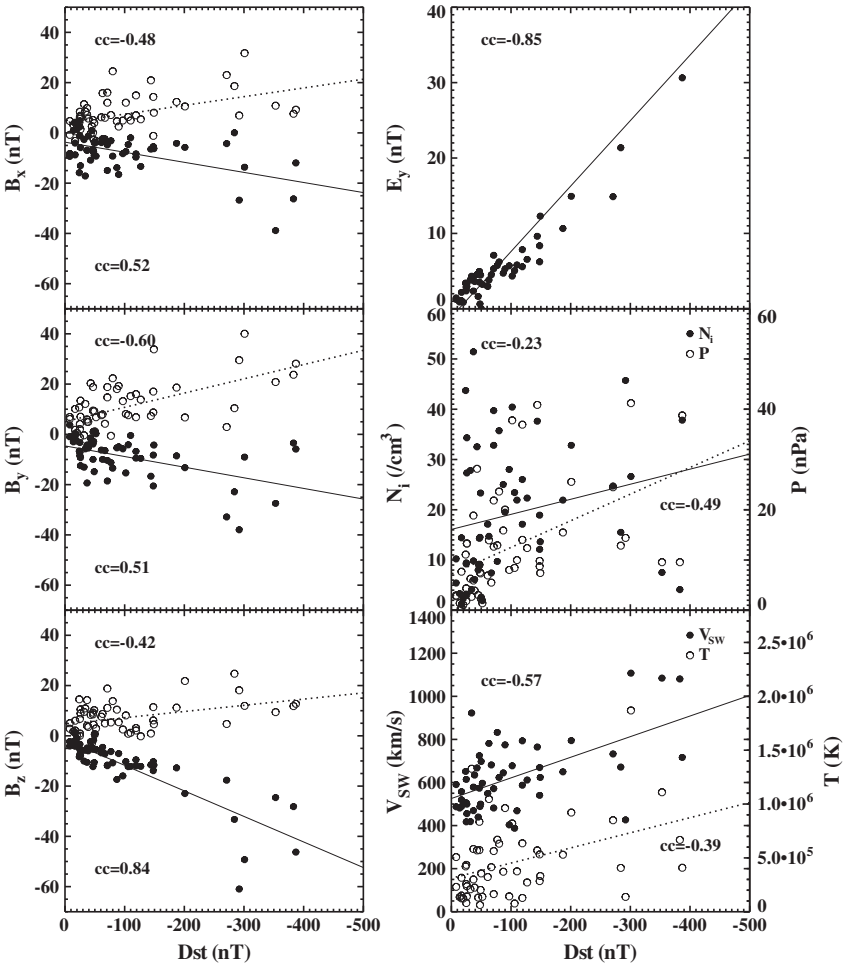

Figure 2. (left column) The relationship between the minimum *Dst* index and magnetic field strengths in the positive direction (open circles) and negative direction (filled circles). (right column) The relationship between the minimum *Dst* index and (top) duskward electric field, (middle) ion number density and flow pressure, and (bottom) solar wind speed and plasma temperature, respectively.

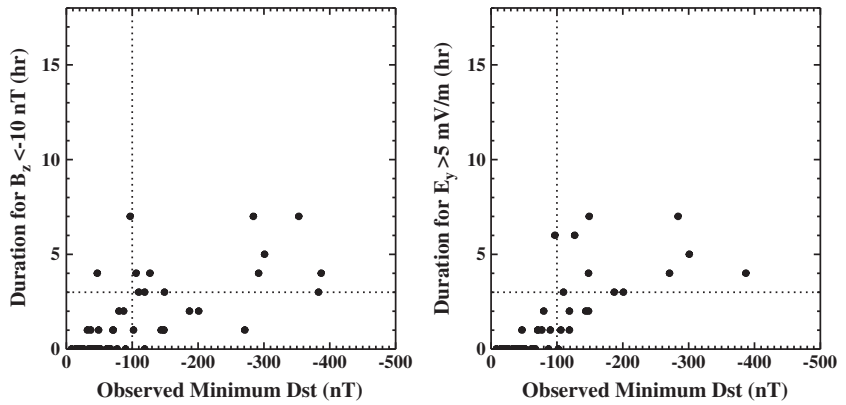

Figure 3. Minimum *Dst* for the storm is plotted against the prior durations of B_z and E_y disturbances in the solar wind. The vertical dotted lines indicate −100 nT, which is a criterion of intense storm, and the horizontal dotted lines indicate the durations of 3 h as in the GT criteria.

Table 2. Storm Prediction Capability According to Each Criteria

B_z (nT)	Duration (h)	<−100 nT PODy	<−100 nT CSI	<−50 nT PODy	<−50 nT CSI	E_y (mV/m)	Duration (h)	<−100 nT PODy	<−100 nT CSI	<−50 nT PODy	<−50 nT CSI
−10	3	0.53	0.50	0.39	0.38	5	3	0.63	0.59	0.39	0.39
	2	0.68	0.62	0.52	0.50		2	0.81	**0.72**	0.54	0.54
−7	3	0.79	**0.68**	0.55	0.53	4	3	0.81	0.68	0.54	0.52
	2	0.95	0.64	0.74	0.66		2	0.94	0.71	0.68	**0.66**
−5	3	0.84	0.57	0.71	0.65	3	3	0.88	0.67	0.64	0.62
	2	**1.00**	0.56	**0.90**	**0.76**		2	**1.00**	0.55	**0.79**	0.63

We also consider the duration of disturbances in solar wind conditions. *Gonzalez and Tsurutani* [1987] analyzed intense geomagnetic storms (minimum *Dst* < −100 nT) for a period of 500 days and suggested critical values of IMF B_z (< −10 nT) and E_y (>5 mV/m) for long duration (> 3 h) as the criteria for intense geomagnetic storms, which is called the GT criteria. In addition to the crucial role of the south component of the magnetic field (B_z) and duskward electric field (E_y), they suggested that long duration is also an important solar wind cause for a storm. Therefore, we measure how long B_z and E_y stay within the GT criteria ($B_z \leq -10$ nT, $E_y \geq 5$ mV/m) before *Dst* minimum. In Figure 3, the vertical dotted lines indicate −100 nT, which is a criterion of intense storm, and the horizontal dotted lines indicate the durations of 3 h as the GT criteria.

3.2. Solar Wind Criteria

However, GT criteria was originally proposed for intense storms; therefore, it may be too strict to distinguish moderate geomagnetic storms, which are the focus of the present study. For example, among 31 storms in our data set, only 12 events satisfy this condition for B_z (12/31, 39%), and 19 storms do not. In a similar

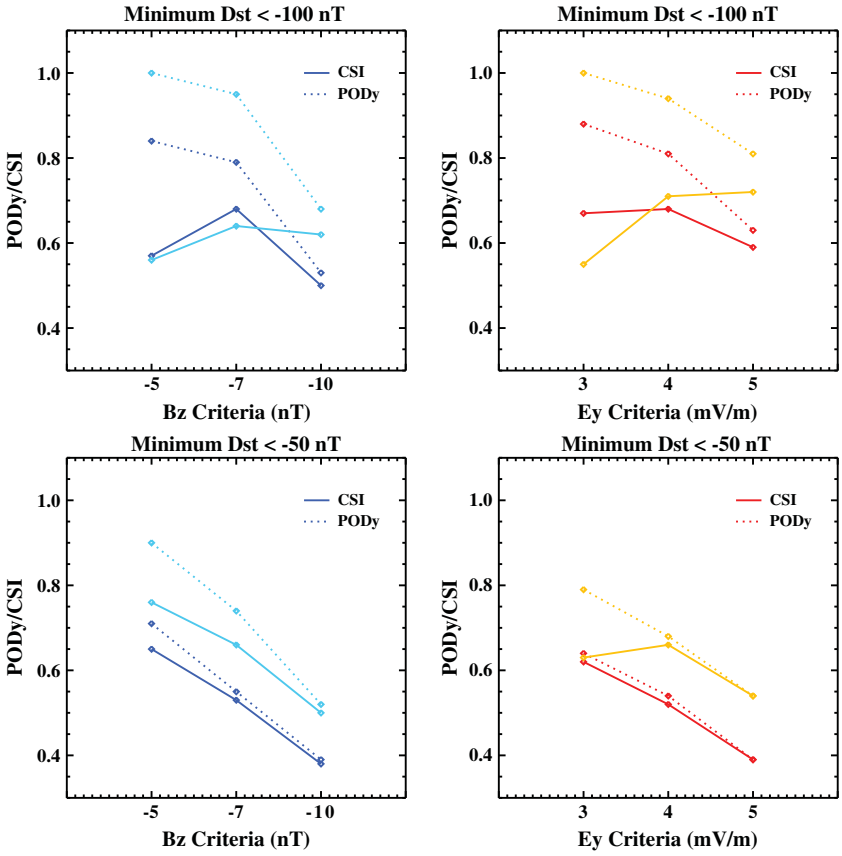

Figure 4. Prediction capabilities (PODy and CSI) according to the disturbances, B_z and E_y, and durations. Blue lines delineate the 3 h duration of B_z disturbances, and sky blue lines are the 2 h durations. Red lines delineate the 3 h duration of E_y disturbances, and orange lines are the 2 h durations.

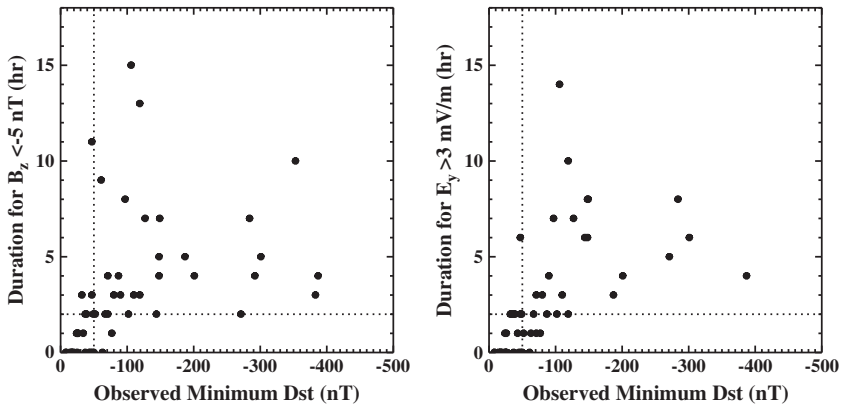

Figure 5. Prior durations of B_z and E_y disturbances according to new solar wind criteria are plotted against minimum *Dst* values for the storms. The vertical dotted lines indicate −50 nT, and the horizontal dotted lines indicate the durations of 2 h.

way, 17 storm events cannot satisfy the E_y condition. Thus, we feel that we need a new solar wind criteria for practical usage in the forecast of moderate storm. To select B_z and E_y criteria as well as their durations for moderate storms, we use contingency tables, which have been widely used in the meteorological forecasting literature. These tables can provide us with information about the success or failure of the forecasting experience. General form and detailed explanation of the contingency table and its statistical parameters can be found in *Smith et al.* [2000]. For several cases of B_z, E_y, and durations, we compared "probability of detection yes (PODy)" and "critical success index (CSI)." PODy is the proportion of correctly forecasted events among the observed storms, and CSI is the proportion of correctly forecasted storm events among those that were either predicted or observed. Table 2 and Figure 4 show PODy and CSI as the storm prediction capabilities according to each criteria. Note that the better forecasts are indicated by statistical values that are closer to 1.0. As shown in the figure, for the moderate storms with the minimum *Dst* less than −50 nT, PODy and CSIs have clear tendency to decrease when the criteria become higher.

In the case of B_z, for intense storms with minimum *Dst* less than −100 nT, CSI is the best (0.68) when we select −7 nT with duration of at least 3 h, as marked by boldface in the table. If we select −5 nT for 2 h as the criteria, PODy is 1.00, which means that we can predict all intense storms, even though there will be many false alarms. For moderate storms with minimum *Dst* less than −50 nT, CSI and PODy are the best when we select −5 nT for 2 h. In the case of E_y, for intense storms, CSI is the best (0.72) when we select 5 mV/m for 2 h. If we select 3 mV/m for 2 h as the criteria, we can predict all intense storms. For moderate storms, CSI and PODy are the best when we select 4 mV/m for 2 h and 3 mV/m for 2 h, respectively.

Therefore, we choose $B_z \leq -5$ nT or $E_y \geq 3$ mV/m for $t \geq 2$ h as new solar wind criteria for moderate storm. Figure 5 shows the durations of modified B_z and E_y criteria. The vertical dotted lines indicate −50 nT, and the horizontal dotted lines indicate the durations of 2 h. Among 31 moderate storms with minimum *Dst* less than −50 nT, 28 events (90%) satisfy these solar wind criteria.

Table 3. Statistical Parameters for the Forecast Evaluations Using CME and Solar Wind Condition

Statistics	CME	SW	TL
Hit	28	28	27
False alarm	12	7	3
Miss	3	3	4
Null	12	17	21
PODy	**0.90**	**0.90**	0.87
PODn	0.50	0.71	**0.88**
FAR	0.30	0.20	**0.10**
Bias	1.29	1.13	**0.97**
CSI	0.65	0.73	**0.79**

3.3. Evaluation of Single-Step Forecasts

Now we have a pair of solar wind criteria (SW) and two predicted *Dst* minimum values from the empirical CME model and the TL model. We evaluate those forecasts and list the statistical results in Table 3. In the table, we mark the best value of each category as a boldface. It is clear that the forecasts using solar wind condition are better than those using only CME parameters, since the former are near-real-time forecasts and the latter are 2–3 days prior forecasts. In the case of PODy, the solar wind criteria produces slightly better forecasts (0.90)

Table 4. Statistical Parameters for the Forecast Evaluations Using CME and Solar Wind Condition

Operator Second Step	CME ∩		CME ∪	
	SW	TL	SW	TL
Hit	25	25	31	30
False alarm	3	2	16	8
Miss	6	6	0	1
Null	21	22	8	16
PODy	0.81	0.81	**1.00**	0.97
PODn	0.88	**0.92**	0.33	0.67
FAR	0.11	**0.07**	0.34	0.21
Bias	**0.90**	0.87	1.52	1.23
CSI	0.74	0.76	0.66	**0.77**

than those based on the TL model (0.87). However, the TL model shows better results for the other quality measures, such as "probability of detection no (PODn)," "false alarm ratio (FAR)," "bias," and CSI. Note that FAR should be closer to 0 for a good forecast. That means that the TL model is more suitable for nonstorm events, since it produces accurate forecasts for 88% of 24 nonstorm events, while the solar wind criteria correctly forecasts only 71% of them. The CSIs for forecasts based on CME parameters, solar wind criteria, and the TL model are 0.65, 0.73, and 0.79, respectively.

4. Two-Step Forecast Using CME and Solar Wind Condition

As listed in Table 3, there are 15 events that are incorrectly forecasted (false alarms + miss) based on CME parameters and 10 and 7 events from solar wind criteria and the TL model, respectively. Among those 15 events, 12 cases (80%) can be properly forecasted based on solar wind criteria or the TL model. In the same way, seven events for the solar wind criteria (70%) and four events for the TL model (57%) can be properly forecasted based on CME conditions. Thus, we combine two storm forecast domains by applying the solar wind criteria and the TL model as the second step.

We consider four cases predicted on the basis of two solar wind domains (solar wind criteria and TL model) and two operators (∩ and ∪) as listed in Table 4. First, we predict a geomagnetic storm only when the event satisfies both CME criteria and solar wind conditions (∩). In both cases of solar wind criteria (CME ∩ SW) and the TL model (CME ∩ TL), only 25 storm events are correctly forecasted (81%) and we miss six storms, which means that the criteria are too strict to improve the forecast capability. If we use the TL model in combination with the CME criteria, the false alarm is less and CSI (0.76) is slightly higher comparing with using the solar wind criteria in combination with the CME criteria (0.74). On the other hand, if we predict a storm when the event satisfies either the CME or solar wind criteria (CME ∪ SW), even though there are many false alarms and CSI (0.66) is not so improved, PODy is 1.00, which means that we do not miss any storms. If we use the TL model instead of the solar wind criteria in the later, CSI (0.77) is the best among those four cases.

5. Summary and Discussion

Since the initially observed CME characteristics can be changed during the transit to the Earth, there are some limitations for forecasts based upon only initial condition from the Sun. On the other hand, if we use only solar wind parameters for the storm forecast, we cannot expect enough preparation time for the storm. To improve the forecast capability for geomagnetic storms, we consider the CME parameters and near real-time solar wind condition together. We use 55 CME-*Dst* pairs associated with M and X class solar flares, which have clearly identifiable source regions during 1997 to 2003. Among the solar wind parameters, we confirm that the peak values of negative B_z and E_y prior to *Dst* minimum are strongly related with the *Dst* index. Then we closely examine the forecast capabilities of those parameters by using contingency tables and select new solar wind criteria. We suggest $B_z \leq -5$ nT or $E_y \geq 3$ mV/m for $t \geq 2$ h as the solar wind criteria for moderate geomagnetic storms with minimum *Dst* less than −50 nT. Among 31 storm events, 90% (28/31) satisfied this criteria producing a CSI of 0.73. We also used the *Dst* model of *Temerin and Li* [2002, 2006] as another solar wind condition. In this case, 87% of storms can be correctly forecasted and CSI is 0.79. Our main results from two-step forecasts of geomagnetic storms by combining two storm forecast domains are as follows.

1. For 15 events that are incorrectly forecasted using only CME parameters, 12 cases (80%) can be properly predicted by solar wind criteria or the TL model.
2. If we predict a geomagnetic storm only when the event satisfies both CME criteria and solar wind condition (∩), CSIs are improved. However, only 25 storm events are correctly forecasted (81%) using either the solar wind criteria (CME ∩ SW) or the TL model (CME ∩ TL).

3. Even though there are many false alarms and CSI (0.66) is not much improved, all storms can be correctly forecasted if we predict a storm when the event satisfies either the CME or solar wind criteria (CME ∪ SW).
4. There is a tendency for the solar wind criteria to give better forecasts for storm events; however, the TL model shows better forecast capability for nonstorm events.

Based on these results, we suggest the two-step forecast of geomagnetic storm. As the first step, we forecast a storm 2–3 days before as soon as we detect a CME with its location, speed, direction parameter, and magnetic field orientation in the source region. Then we update the storm forecast after monitoring the arrival of the CME/ICME near Earth as the second step. We adopt our new solar wind criteria and the TL model as the second step of the geomagnetic storm forecast. Our result shows a sufficient possibility for improving the geomagnetic storm prediction by updating with the real-time forecast. However, we need to think about which forecast based on solar wind parameters is better, one based on solar wind criteria or the TL model, and also which operator, cap or cup (∩ or ∪), will be better for practical usage. For a higher critical success index, the TL model and cap operator are better, but for the prediction of storm events, the solar wind criteria and cup operator can give better forecasts.

Recently, *Uwamahoro et al.* [2012] estimated the geoeffectiveness of halo CMEs from associated solar and IP parameters using neural networks. They presented an improved performance with an accuracy of 86% in the prediction of geomagnetic storm occurrence. We emphasize that our two-step forecast can predict the storm strength also, since we use the empirical forecast formulae based on CME parameters as the first step. The calculated values from the formulae have good correlations with the observed *Dst* values for northward oriented overlying fields in the CME source region (cc = 0.80) but less so for southward oriented cases (cc = 0.66). This may imply that there are other factors for the southward events, which is not well understood. Further studies on the evolution of CME's magnetic fields during its passage from the Sun to the Earth and the interaction with the geomagnetic fields are needed.

Acknowledgments
We thank the referees for careful reading of the manuscript and valuable suggestions and criticism that led to significant improvement of the paper. This work was supported by the Construction of Korean Space Weather Center as the project of KASI, the KASI Basic Research Fund, and Research Fellowship for Young Scientists of KRCF. Y.-J.M. has been supported by the WCU program (R31-10016) and Basic Research Promotion Fund (20090071744 and 20100014501) through the National Research Foundation of Korea funded by the Ministry of Education, Science, and Technology.

References

Bothmer, V., and R. Schwenn (1998), The structure and origin of magnetic clouds in the solar wind, *Ann. Geophys.*, *16*, 1–24.
Boynton, R. J., M. A. Balikhin, S. A. Billings, H. L. Wei, and N. Ganushkina (2011), Using the NARMAX OLS-ERR algorithm to obtain the most influential coupling functions that affect the evolution of the magnetosphere, *J. Geophys. Res.*, *116*, A05218, doi:10.1029/2010JA015505.
Brueckner, G. E., et al. (1995), The large angle spectroscopic coronagraph (LASCO), *Sol. Phys.*, *162*, 357–402.
Brueckner, G. E., J.-P. Delaboudiniere, R. A. Howard, S. E. Paswaters, O. C. St. Cyr, R. Schwenn, P. Lamy, G. M. Simnett, B. Thompson, and D. Wang (1998), Geomagnetic storms caused by coronal mass ejections (CMEs): March 1996 through June 1997, *Geophys. Res. Lett.*, *25*, 3019–3022.
Burton, R. K., R. L. McPherron, and C. T. Russell (1975), An empirical relationship between interplanetary conditions and Dst, *J. Geophys. Res.*, *80*, 4204–4214.
Cho, K.-S., Y.-J. Moon, M. Dryer, C. D. Fry, Y.-D. Park, and K.-S. Kim (2003), A statistical comparison of interplanetary shock and CME propagation models, *J. Geophys. Res.*, *108*(A12), 1445, doi:10.1029/2003JA010029.
Cho, K.-S., S.-C. Bong, Y.-J. Moon, M. Dryer, S.-E. Lee, and K.-H. Kim (2010), An empirical relationship between coronal mass ejection initial speed and solar wind dynamic pressure, *J. Geophys. Res.*, *115*, A10111, doi:10.1029/2009JA015139.
Echer, E., W. D. Gonzalez, and B. T. Tsurutani (2008), Interplanetary conditions leading to superintense geomagnetic storms (Dst ≤ −250 nT) during solar cycle 23, *Geophys. Res. Lett.*, *35*, L06S03, doi:10.1029/2007GL031755.
Fenrich, F. R., and J. G. Luhmann (1998), Geomagnetic response to magnetic clouds of different polarity, *Geophys. Res. Lett.*, *25*, 2999–3002.
Gonzalez, W. D., and B. T. Tsurutani (1987), Criteria of interplanetary parameters causing intense magnetic storms (Dst < −100 nT), *Planet. Space Sci.*, *35*, 1101–1109.
Gonzalez, W. D., J. A. Joselyn, Y. Kamide, H. W. Kroehl, G. Rostoker, B. T. Tsurutani, and V. M. Vasyliunas (1994), What is a geomagnetic storm?, *J. Geophys. Res.*, *99*, 5771–5792.
Gopalswamy, N., A. Lara, R. P. Lepping, M. L. Kaiser, D. Berdichevsky, and O. C. St. Cyr (2000), Interplanetary acceleration of coronal mass ejections, *Geophys. Res. Lett.*, *27*, 145–148.
Gopalswamy, N., A. Lara, S. Yashiro, M. Kaiser, and R. A. Howard (2001), Predicting the 1-AU arrival times of coronal mass ejections, *J. Geophys. Res.*, *106*, 29,207–29,217.
Ji, E.-Y., Y.-J. Moon, K.-H. Kim, and D.-H. Lee (2010), Statistical comparison of interplanetary conditions causing intense geomagnetic storms (Dst ≤ −100 nT), *J. Geophys. Res.*, *115*, A10232, doi:10.1029/2009JA015112.
Ji, E.-Y., Y.-J. Moon, N. Gopalswamy, and D.-H. Lee (2012), Comparison of Dst forecast models for intense geomagnetic storms, *J. Geophys. Res.*, *117*, A03209, doi:10.1029/2011JA016872.
Kang, S.-M., Y.-J. Moon, K.-S. Cho, Y.-H. Kim, Y. D. Park, J.-H. Baek, and H.-Y. Chang (2006), Coronal mass ejection geoeffectiveness depending on field orientation and interplanetary coronal mass ejection classification, *J. Geophys. Res.*, *111*, A05102, doi:10.1029/2005JA011445.
Kim, K.-H., Y.-J. Moon, and K.-S. Cho (2007), Prediction of the 1-AU arrival times of CME-associated interplanetary shocks: Evaluation of an empirical interplanetary shock propagation model, *J. Geophys. Res.*, *112*, A05104, doi:10.1029/2006JA011904.
Kim, R.-S., K.-S. Cho, Y.-J. Moon, Y.-H. Kim, Y. Yi, M. Dryer, S.-C. Bong, and Y.-D. Park (2005), Forecast evaluation of the coronal mass ejection (CME) geoeffectiveness using halo CMEs from 1997 to 2003, *J. Geophys. Res.*, *110*, A11104, doi:10.1029/2005JA011218.

Kim, R.-S., K.-S. Cho, K.-H. Kim, Y.-D. Park, Y.-J. Moon, Y. Yi, J. Lee, H. Wang, H. Song, and M. Dryer (2008), CME earthward direction as an important geoeffectiveness indicator, *Astrophys. J.*, *677*, 1378.

Kim, R.-S., K.-S. Cho, Y.-J. Moon, M. Dryer, J. Lee, Y. Yi, K.-H. Kim, H. Wang, Y.-D. Park, and Y.-H. Kim (2010), An empirical model for prediction of geomagnetic storms using initially observed CME parameters at the Sun, *J. Geophys. Res.*, *115*, A12108, doi:10.1029/2010JA015322.

King, J. H., and N. E. Papitashvili (2005), Solar wind spatial scales in and comparisons of hourly Wind and ACE plasma and magnetic field data, *J. Geophys. Res.*, *110*, A02104, doi:10.1029/2004JA010649.

McKenna-Lawlor, S. M. P., M. Dryer, M. D. Kartalev, Z. Smith, C. D. Fry, W. Sun, C. S. Deehr, K. Kecskemety, and K. Kudela (2006), Near real-time predictions of the arrival at Earth of flare-related shocks during Solar Cycle 23, *J. Geophys. Res.*, *111*, A11103, doi:10.1029/2005JA011162.

Moon, Y.-J., M. Dryer, Z. Smith, Y.-D. Park, and K.-S. Cho (2002), A revised shock time of arrival (STOA) model for interplanetary shock propagation: STOA-2, *Geophys. Res. Lett.*, *29*(10), 1390, doi:10.1029/2002GL014865.

Moon, Y.-J., K.-S. Cho, M. Dryer, Y.-H. Kim, S.-C. Bong, J. Chae, and Y.-D. Park (2005), New geoeffective parameters of very fast halo coronal mass ejections, *Astrophys. J.*, *624*, 414–419.

Moon, Y.-J., R.-S. Kim, and K.-S. Cho (2009), Geometrical implication of the CME earthward direction parameter and its comparison with cone model parameters, *J. Korean Astron. Soc.*, *42*, 27–32.

O'Brien, T. P., and R. L. McPherron (2000), An empirical phase space analysis of ring current dynamics: Solar wind control of injection and decay, *J. Geophys. Res.*, *105*, 7707–7719.

Schwenn, R. (2006), Space weather: The solar perspective, *Living Rev. Sol. Phys.*, *3*, 2, doi:10.12942/lrsp-2006-2.

Smith, Z., M. Dryer, E. Ort, and W. Murtagh (2000), Performance of interplanetary shock prediction models: STOA and ISPM, *J. Atmos. Sol. Terr. Phys.*, *62*, 1265–1274.

Song, H., V. Yurchyshyn, G. Yang, C. Tan, W. Chen, and H. Wang (2006), The automatic predictability of super geomagnetic storms from halo CMEs associated with large solar flares, *Sol. Phys.*, *238*, 141–165.

Srivastava, N., and P. Venkatakrishnan (2004), Solar and interplanetary sources of major geomagnetic storms during 1996–2002, *J. Geophys. Res.*, *109*, A10103, doi:10.1029/2003JA010175.

Temerin, M., and X. Li (2002), A new model for the prediction of Dst on the basis of the solar wind, *J. Geophys. Res.*, *107*(A12), 1472, doi:10.1029/2001JA007532.

Temerin, M., and X. Li (2006), Dst model for 1995–2002, *J. Geophys. Res.*, *111*, A04221, doi:10.1029/2005JA011257.

Uwamahoro, J., L. A. McKinnell, and J. B. Habarulema (2012), Estimating the geoeffectiveness of halo CMEs from associated solar and IP parameters using neural networks, *Ann. Geophys.*, *30*, 963–972.

Wang, C. B., J. K. Chao, and C.-H. Lin (2003), Influence of the solar wind dynamic pressure on the decay and injection of the ring current, *J. Geophys. Res.*, *108*(A9), 1341, doi:10.1029/2003JA009851.

Wu, C.-C., and R. P. Lepping (2002), Effects of magnetic clouds on the occurrence of geomagnetic storms: The first 4 years of Wind, *J. Geophys. Res.*, *107*(A10), 1314, doi:10.1029/2001JA000161.

Yashiro, S., N. Gopalswamy, G. Michalek, O. C. St. Cyr, S. P. Plunkett, N. B. Rich, and R. A. Howard (2004), A catalog of white light coronal mass ejections observed by the SOHO spacecraft, *J. Geophys. Res.*, *109*, A07105, doi:10.1029/2003JA010282.

Yermolaev, Yu. I., Yu. M. Yermolaev, I. G. Lodkina, and N. S. Nikolaeva (2007), Statistical investigation of Heliospheric conditions resulting in magnetic storms: 2, *Cosmic Res.*, *45*(6), 461–470.

Yurchyshyn, V., V. Abramenko, and D. Tripathi (2009), Rotation of white-light coronal mass ejection structures as inferred from LASCO coronagraph, *Astrophys. J.*, *705*, 426–435.

Zhang, J.-C., M. W. Liemohn, J. U. Kozyra, M. F. Thomsen, H. A. Elliott, and J. M. Weygand (2006), A statistical comparison of solar wind sources of moderate and intense geomagnetic storms at solar minimum and maximum, *J. Geophys. Res.*, *111*, A01104, doi:10.1029/2005JA011065.